A Monoclonal Antibody Against $\alpha_V\beta_3$ Integrin Inhibits Development of Atherosclerotic Lesions in Diabetic Pigs

Laura A. Maile[1], **Walker H. Busby**[1], **Timothy C. Nichols**[2], **Dwight A. Bellinger**[3], **Elizabeth P. Merricks**[2], **Michael Rowland**[1], **Umadevi Veluvolu**[1], and **David R. Clemmons**[1,*]

[1]Division of Endocrinology, University of North Carolina, Chapel Hill, NC 27599-7170, USA

[2]Department of Pathology and Laboratory Medicine, University of North Carolina, Chapel Hill, NC 27599-7170, USA

[3]Division of Laboratory Animal Medicine, University of North Carolina, Chapel Hill, NC 27599-7170, USA

Abstract

Atherosclerotic lesions develop and progress more rapidly in diabetic patients than in nondiabetic individuals. This may be caused by accelerated lesion formation in the high-glucose environment of diabetes. Smooth muscle cells (SMCs) cultured in high glucose are more responsive to growth factors such as insulin-like growth factor–1 (IGF-1). This enhanced response to IGF-1 is due in part to increased activation of the $\alpha_V\beta_3$ integrin. We tested whether $\alpha_V\beta_3$ integrin activation was increased in diabetic animals and whether an antibody to β_3 would inhibit IGF-1 action and development of atherosclerosis. Eight male pigs were made diabetic with streptozotocin and fed a high-fat diet. A F(ab)$_2$ antibody fragment directed at β_3 was infused into one femoral artery, whereas the other artery received control F(ab)$_2$ for 3.5 months. There was a $65 \pm 8\%$ reduction in atherosclerotic lesion area in the arteries treated with F(ab)$_2$ antibody to β_3. Phosphorylation of β_3 was reduced by $75 \pm 18\%$ in vessels treated with the antibody. Shc and mitogen-activated protein kinase phosphorylation, which are required for IGF-1–stimulated SMC proliferation, were also significantly reduced. We conclude that activation of IGF-1 receptor and $\alpha_V\beta_3$-linked signaling pathways accelerates atherosclerosis in diabetes and that administration of an antibody to β_3 to diabetic pigs inhibits $\alpha_V\beta_3$ activation, IGF-1–stimulated signaling, and atherosclerotic lesion development. This approach offers a potential therapeutic approach to the treatment of this disorder.

INTRODUCTION

Atherosclerosis is the leading cause of death for patients with both type 1 and type 2 diabetes (1). Despite the success of therapies that modify hypertension and hypercholesterolemia, treatments that target the accelerated rate of atherosclerosis that occurs in response to chronic hyperglycemia are not available (2). Insulin-like growth factor–1 (IGF-1) stimulates the proliferative phase of atherosclerosis, suggesting that inhibiting IGF-1 could prevent lesion progression (3–6). However, because IGF-1 inhibits apoptosis in neural tissue, cartilage, and skeletal muscle, targeting the IGF-1 receptor could lead to unacceptable toxicity (7, 8). Consequently, there is a need for a more selective way to inhibit IGF-1 action.

In contrast to the IGF-1 receptor, expression of $\alpha_V\beta_3$ integrin is limited to three cell types: endothelium, smooth muscle, and osteoclasts. The abundance of $\alpha_V\beta_3$ is increased in atherosclerotic lesions, and ligands for $\alpha_V\beta_3$, such as osteopontin and thrombospondin, are also increased in arteries from diabetic animals (9–12). Interaction between the IGF-1 receptor and $\alpha_V\beta_3$-linked signaling pathways enhances IGF-1–stimulated smooth muscle cell (SMC) growth and migration in vitro (13), and SMCs only migrate in response to IGF-1 when $\alpha_V\beta_3$ ligands are also present in the culture medium. Hyperglycemia causes increased cellular secretion of $\alpha_V\beta_3$ ligands, which enhance the sensitivity of SMCs to stimulation by IGF-1 (11, 12, 14). Blocking ligand occupancy with an antibody or peptide antagonist that binds to $\alpha_V\beta_3$ inhibits IGF-1–stimulated proliferation of SMCs in hyperglycemia (13–15). Several investigators have targeted, with antibodies and inhibitory peptides, the binding site on $\alpha_V\beta_3$ for Arg-Gly-Asp (RGD) sequences of $\alpha_V\beta_3$ ligands (16–18). These RGD antagonists can have effects other than inhibition of ligand actions. These include partial agonist activity, $\alpha_V\beta_3$ conformational-dependent changes that alter the cellular response to the antagonist, and binding of the antagonist to other sites on $\alpha_V\beta_3$ that can modify its inhibitory actions (18–20). One region of $\alpha_V\beta_3$, referred to as the cysteine loop (C-loop) region (21), is distinct from the RGD-binding site (22) and interacts with the heparin-binding domain of vitronectin, a glycoprotein of the extracellular matrix (23). This interaction is required for $\alpha_V\beta_3$ ligands to enhance the response of SMCs to IGF-1 stimulation in vitro, but ligand binding through the RGD-binding site does not activate this pathway (20, 23). Therefore, targeting the C-loop region may inhibit IGF-1 signaling without triggering the negative effects of RGD-binding site antagonists. Because all previous studies have analyzed this interaction in vitro, we undertook this study to determine in vivo the efficacy of a monoclonal antibody that reacts specifically with the C-loop region. We tested whether the interaction could inhibit atherosclerotic lesion progression in a porcine model of hyperglycemia-accelerated atherosclerosis.

RESULTS

Inhibition of β_3 subunit phosphorylation and IGF-1 signaling in cultured SMCs by F(ab)$_2$ antibody to β_3

The addition of vitronectin to cultured SMC resulted in a 5.2 ± 2.4–fold (mean ± SEM, $P < 0.01$) increase in β_3 phosphorylation, which was completely inhibited by the purified F(ab)$_2$ (10^{-9} M) (Fig. 1A and fig. S1A). IGF-1 stimulated Shc phosphorylation 5.7 ± 0.5–fold, but this increase was reduced to 2.9 ± 0.4–fold after exposure to F(ab)$_2$ antibody to β_3 (mean ± SEM, $n = 3$, $P < 0.01$) (Fig. 1B and fig. S1B). Grb-2 recruitment to Shc was reduced from 3.8 ± 0.4–fold to 2.0 ± 0.5–fold (mean ± SEM, $n = 3$, $P < 0.05$). Phosphorylation of extracellular signal–regulated kinase 1/2 (ERK1/2) was increased 7.6 ± 0.8–fold after 5 min in response to IGF-1 relative to a 2.0 ± 0.2–fold increase in cultures exposed to F(ab)$_2$ (mean ± SEM, $n = 3$, $P < 0.01$) (Fig. 1C and fig. S1C). IGF-1 increased cell number by a

factor of 2.5, and this response was reduced significantly by the antibody (Fig. 1D and fig. S1D).

Long-term infusion of F(ab)$_2$ antibody to β$_3$ and its effects on lesion progression

As for our in vitro experiments, analysis of aortic extracts from diabetic and control pigs showed that β$_3$ phosphorylation was markedly increased in the arteries from diabetic animals ($P < 0.001$) (fig. S2). After treatment with streptozotocin, all of the animals became hyperglycemic and mean glucose (four values per 24-hour period) increased from 62 ± 6 mg/dl to 340 ± 94 mg/dl (Table 1). Six of eight animals required daily insulin administration to maintain glucose at <450 mg/dl. Mean glucose values ranged from 340 to 368 mg/dl (Table 1). Weight increased progressively, which is typical for growing animals in this age range. Both cholesterol and triglyceride concentrations were significantly increased in response to the high-fat diet and the induction of diabetes.

To determine whether the infused C-loop F(ab)$_2$ altered lesion progression, we compared the area of atherosclerotic lesions from those arteries to control F(ab)$_2$–treated arteries. The analyses show that arteries that received control F(ab)$_2$ developed atherosclerotic lesions (Fig. 2, top row). Histologic evaluation shows increased neointimal formation and lipid deposition with foam cells and a fibrous cap. Representative sections from a control F(ab)$_2$–treated artery from a second animal show a large proliferation lesion and similar histologic changes (Fig. 2, second row). Sections from the contralateral artery from the same animal that received F(ab)$_2$ antibody to β$_3$ show a marked reduction in lesion size (Fig. 2, fourth row). Staining for macrophages shows that they are present in the neointima of the control F(ab)$_2$–treated artery (Fig. 2, third row). The sections from the artery that received the F(ab)$_2$ antibody to β$_3$ show minimal macrophage accumulation (Fig. 2, fifth row) The mean intimal area of the eight vessels that received F(ab)$_2$ antibody to β$_3$ was reduced by $68 \pm 11\%$ when compared to controls (Table 2). Intimal area expressed as the percentage of the medial area was also significantly reduced (Table 2).

Proliferating cell nuclear antigen (PCNA) labeling showed that fewer, $9 \pm 6\%$ of cells, were labeled in vessels treated with F(ab)$_2$ antibody to β$_3$ relative to control (for example, $19 \pm 3.7\%$) ($P < 0.01$) (Table 2). These findings support the conclusion that the reduction in neointimal area is due in large part to a reduction in cell growth.

Effect of long-term infusion of F(ab)$_2$ antibody to β$_3$ on IGF-1–mediated signaling events

The F(ab)$_2$ antibody to β$_3$ reduced β$_3$ phosphorylation by $75 \pm 18\%$ (mean $\pm$ SD, $n = 8$, $P < 0.01$) (Fig. 3). Representative data from two antibody and two control-treated arteries are shown in Fig. 3. Antibody treatment also reduced Shc association with SHPS-1 ($49 \pm 12\%$) and Shc phosphorylation ($79 \pm 20\%$). C-loop antibody exposure reduced phospho–mitogen-activated protein kinase (MAPK) by $71 \pm 9\%$. To determine whether IGF-1–stimulated signaling had been inhibited, we analyzed the arterial homogenates for IGF-binding protein–5 (IGFBP-5), a protein whose synthesis is stimulated by IGF-1. Exposure to the antibody resulted in a $67 \pm 13\%$ decrease in IGFBP-5 (mean $\pm$ SEM, $n = 8$, $P < 0.01$).

Extraction of the lesions and measurement of the antibody concentrations showed that the arteries that received the F(ab)$_2$ antibody to β$_3$ had a mean concentration of $9.6 \pm 2.4 \times 10^{-9}$ M (mean $\pm$ SEM, $n = 8$). The F(ab)$_2$ concentrations in the vessels that received control F(ab)$_2$ was $1.4 \pm 0.2 \times 10^{-8}$ M. The concentration of F(ab)$_2$ antibody to β$_3$ in serum from the animals was below the limit of detection of the assay ($<1.9 \times 10^{-10}$ M).

DISCUSSION

The results of this study show that administration of the F(ab)$_2$ fragment of a monoclonal antibody that binds to a specific domain on the β_3 subunit of the $\alpha_V\beta_3$ integrin (the C-loop region) inhibits atherosclerotic lesion progression when administered locally to hypercholesterolemic diabetic pigs. The effect of the antibody was due in part to inhibition of cell proliferation, although an effect on extracellular matrix accumulation and cell migration cannot be excluded. To confirm that the difference in lesion progression was due to inhibition of IGF-1–$\alpha_V\beta_3$ signaling, we assessed the activation state of signaling pathway components that are increased when cultured vascular SMCs are exposed to IGF-1 and hyperglycemia. The F(ab)$_2$ antibody to β_3 fragment inhibited β_3 phosphorylation, which is activated in lesion tissue in response to increases in $\alpha_V\beta_3$ ligands, such as osteopontin and thrombospondin. The abundance of these ligands is increased in response to hyperglycemia. Treatment with the F(ab)$_2$ antibody to β_3 also inhibited phosphorylation of signaling components such as Shc and MAPK, which are stimulated in vascular SMCs in response to $\alpha_V\beta_3$ and IGF-1 receptor stimulation and mediate increased SMC migration and proliferation in vitro (14). Our results indicate that the concentrations of the F(ab)$_2$ antibody to β_3 that were achieved in vivo were sufficient to suppress activation of these signaling components. Because the antibody also inhibited atherosclerotic lesion progression significantly, the results suggest that blocking the activation of $\alpha_V\beta_3$ in diabetic pigs results in attenuation of lesion growth.

Previous studies have shown that $\alpha_V\beta_3$ is activated after vascular injury (for example, balloon denudation) in mice (9). Similarly, an $\alpha_V\beta_3$ monoclonal antibody that inhibited injury-induced activation attenuated lesion formation (16) and $\beta_3^{-/-}$ mice had reduced neointimal lesion formation in response to carotid artery injury (24). A study with a vascular stenosis model demonstrated that an $\alpha_V\beta_3$ antagonist attenuated neointimal expansion in pigs (17). β_3-Integrins are up-regulated after vascular injury in baboons, and β_3 up-regulation enhances the SMC response to thrombospondin or thrombin (25). Growth factors that stimulate SMC growth, such as transforming growth factor–β and platelet-derived growth factor (PDGF)–BB, enhance β_3 expression (26). Two different $\alpha_V\beta_3$ monoclonal antibodies inhibited human coronary SMC migration (27). Furthermore, treatment of patients undergoing angioplasty and stent placement with abciximab (a monoclonal antibody that binds to αIIB β_3) decreases the need for revascularization (28). Our results show that inhibiting ligand binding to $\alpha_V\beta_3$ inhibits lesion progression in a diabetic animal model, extending previous work to a model in which progression of atherosclerosis is exacerbated by chronic hyperglycemia.

The mechanisms by which hyperglycemia leads to $\alpha_V\beta_3$ activation are not well characterized. Endothelial cells that express $\alpha_V\beta_3$ are stimulated to migrate in the presence of hyperglycemia (29), and $\alpha_V\beta_3$ expression is up-regulated in endothelium and microvascular SMC in diabetes (30, 31). The ligands that bind to $\alpha_V\beta_3$ are also up-regulated. Osteopontin concentrations are increased in tissues from diabetic animals, as are thrombospondin and connective tissue growth factor (32–35), and vascular SMCs in culture exposed to hyperglycemia secrete increased amounts of thrombospondin, osteopontin, and vitronectin (14). That the increase in $\alpha_V\beta_3$ ligands is functionally relevant is demonstrated by our observation that β_3 phosphorylation is constitutively increased in arteries from diabetic pigs (fig. S2). The importance of β_3 phosphorylation was proven by mutating the two key tyrosines in its cytoplasmic domain and showing that SMCs expressing that mutant were refractory to the sensitizing effect of hyperglycemia on IGF-1–stimulated cell proliferation (36). This activation of β_3 is mediated by binding the C-loop domain (21). Indeed, our data show that the monoclonal antibody used in this study inhibits the ability of IGF-1 to stimulate Shc and MAPK phosphorylation, as well as cellular proliferation (Fig. 1).

Other investigators have demonstrated that antibodies to $\alpha_V\beta_3$ inhibit mesangial and SMC growth or migration in vitro in response to hypoxia plus hyperglycemia (37). Although the responses to other growth factors are enhanced in the presence of hyperglycemia, this occurs by different mechanisms. For example, hyperglycemia enhances the ability of PDGF to stimulate autophosphorylation of the PDGF receptor, which leads to mitogenesis (38), but this response does not depend on $\alpha_V\beta_3$ ligand occupancy.

After mechanical injury (denudation of the interior wall of the vasculature with a balloon catheter), vascular cells show an increase in IGF-1 synthesis (39, 40), and overexpression of IGF-1 by SMC results in an enhanced proliferative response to balloon injury (3). Similarly, somatostatin analogs, which decrease IGF-1 synthesis by SMC, inhibit human coronary SMC proliferation (41). In contrast, previous in vitro studies showed that hyperglycemia enhances IGF-1 signaling responses via increased ligand occupancy of $\alpha_V\beta_3$ but that there is no alteration in IGF-1 receptor abundance or in its activation (14). Our study shows that, if only $\alpha_V\beta_3$ and not the IGF-1 receptor is inhibited, both neointimal lesion size and IGF-1 signaling are reduced. These results suggest that chronic activation of $\alpha_V\beta_3$ is required to enhance cellular signaling in response to IGF-1 and that this activation stimulates cellular accumulation in the neointima. Our results do not exclude the possibility that inhibiting IGF-1 receptors would also contribute to attenuation of atherosclerotic lesion formation, but they do suggest that when hyperglycemia is present interrupting only one limb of the pathway is adequate for lesion inhibition. Because $\alpha_V\beta_3$ functions cooperatively by enhancing response to IGF-1 during hyperglycemia, this antibody provides a useful research tool for examining whether it can reduce the sensitivity of vascular cells to IGF-1 to a level that approximates their normal physiologic response to IGF-1 stimulation.

Hormones that induce stress in vascular wall cell types, such as angiotensin II and aldosterone, increase IGF-1 receptor synthesis (42). A stable peptide analog of IGF-1 that inhibited IGF-1 binding to the IGF-1 receptor inhibited SMC proliferation after balloon injury in the rat (43). These findings suggest that it would be logical to target the IGF-1 receptor directly to inhibit atherosclerosis. However, because IGF-1 receptors are expressed ubiquitously, this approach could lead to other deleterious effects. IGF-1 has anabolic and antiapoptotic effects in skeletal muscle, bone, and brain (44). Furthermore, inhibitors of the IGF-1 receptor tyrosine kinase also inhibit the insulin receptor tyrosine kinase, which could exacerbate deteriorating glucose control (45). Therefore, our strategy to target $\alpha_V\beta_3$, an integrin co-receptor that is expressed in only three cell types, reduces the risk of inducing these unwanted responses. Nevertheless, even an antibody with this narrow spectrum of activity could induce side effects (for example, inhibition of bone resorption or inhibition of premenstrual angiogenesis in the uterus). These potential side effects would need to be investigated before clinical application.

In addition to potential off-target effects, several questions need to be addressed before translation of these findings to the treatment of humans with atherosclerosis. Initially, it will be important to determine whether the antibody can inhibit atherosclerosis in patients with diabetes who do not have hyperlipidemia. Selection of the appropriate patient population for analysis (for example, patients with established atherosclerosis and proliferative disease) will also be important. Finally because IGF-1 also has antiapoptotic effects and rapid induction of apoptosis has been proposed to lead to plaque rupture (46), patients who are being treated with integrin inhibition will need to be carefully monitored for this potential complication.

Our studies demonstrate that blocking ligand binding to the C-loop region of $\alpha_V\beta_3$ results in attenuation of the accelerated atherosclerosis that occurs in a porcine model of diabetic atherosclerosis. These effects are mediated in part by blocking the hyperglycemia-induced

enhancement of cellular responsiveness to IGF-1. Inhibiting the $\alpha_V\beta_3$ receptor with a monoclonal antibody that binds to a specific site on the β_3 subunit is a promising approach for treatment of proliferative phase of this disease in patients with diabetes.

MATERIALS AND METHODS

Materials

Polyvinyl difluoride membranes (Immobilon P) were purchased from Millipore. Autoradiographic film was from Pierce. Fetal bovine serum, Dulbecco's modified Eagle's medium (DMEM), penicillin, and streptomycin were from Life Technologies. The phosphotyrosine antibody (PY99) was from Santa Cruz Biotechnology. The polyclonal antibody against β_3 was prepared as described (14). Phospho-ERK1/2, total ERK1/2, and antibodies to Grb-2 and Shc were from BD Transduction Laboratories. The antibody to SHPS-1 was from Upstate. Secondary antibodies were from Jackson ImmunoResearch. All other reagents were purchased from Sigma Chemical unless otherwise stated. Porcine aortic SMCs were isolated and maintained in 4.5 g of DMEM per liter of glucose (47). Cells were used between passage 5 and passage 16.

Generation and purification of the monoclonal C-loop antibody to β_3 and the F(ab)$_2$ fragment

Four BALB/c mice were immunized with a peptide immunogen–keyhole limpet hemocyanin (KLH) conjugate (23). A high-producing monoclonal antibody clone was generated and selected (14). The clone was expanded in medium containing 10% low immunoglobulin G (IgG) (Gibco) serum, interleukin-6 bovine (10 μg/ml) (Roche), glutamine (4 mM), penicillin (500 U/ml), and streptomycin (200 μg/ml) (Gibco) to a density of 2.5×10^5 cells/ml; transferred to 2-liter roller bottles; and maintained at that density by adding fresh media every 48 hours until the volume reached 600 ml. A total of 10 l of conditioned medium, which contained 720 mg of the antibody, was collected and then concentrated by ammonium sulfate precipitation.

The enzyme ficin linked to agarose (200 ml) (Pierce-Thermo Fisher) was washed and activated (48). The ficin agarose was incubated with the ammonia sulfate precipitate (3 mg/ml) for 96 hours at 37°C. After incubation, the digested IgG was applied to a protein A affinity column to remove noncleaved, intact IgG and Fc fragment. The flow-through material containing F(ab)$_2$ was purified by protein G–Sepharose followed by an affinity column that had been prepared by conjugating the C-loop domain peptide to Sepharose. The material was eluted in 0.5 M Na$_2$PO$_4$ (pH 3.0) and then analyzed by SDS–polyacrylamide gel electrophoresis (PAGE) with immunoblotting for IgG as well as silver staining. A single band (molecular weight estimate of 120 kD) was detected. Immunoblotting confirmed that it was a F(ab)$_2$ fragment. Immunoblotting with Fc antibodies showed that >99.6% of the Fc fragment was removed and <0.1% of intact IgG remained. The recovery was 42%. The affinity as calculated by Scatchard analysis was 1.2×10^9. The F(ab)$_2$ fragment from the control antibody prepared by immunizing mice with KLH was purified using the same method.

Enzyme-linked immunosorbent assay method

A 96-well Immulon IV plate (Fisher) was coated with CYDMKTTC immunogen peptide (50 μg/ml) conjugated to bovine serum albumin (BSA). After washing (0.05% Tween) and blocking (2% BSA), the samples were added and incubated for 1 hour at 22°C. An alkaline phosphatase–conjugated secondary antibody (goat antibody to mouse; Jackson ImmunoResearch) was added followed by diethanolamine developer (50 μl per well)

containing *p*-nitrophenyl phosphate for 15 min, and the results were determined by spectrophotometry at 405 nm.

Testing of purified β₃ C-loop F(ab)₂ antibody

Quiescent SMCs (5×10^6 cells per 10-cm dish) were incubated in serum-free medium and 02% BSA overnight. Control or β_3 C-loop F(ab)$_2$ (10^{-9} M) was added for 4 hours followed by IGF-1 (50 ng/ml). To examine β_3 phosphorylation, we added vitronectin (1 µg/ml) 3 hours after addition of the antibody and the incubation continued for 60 min. SMCs were lysed in modified radioimmunoprecipitation assay (RIPA) buffer and analyzed by immunoblotting with the appropriate antibody (14). For immunoprecipitation studies, cell lysates were incubated overnight at 4°C with the appropriate antibody (for example, β_3 or Shc), immune complexes were precipitated with protein A–Sepharose, the pellets were resuspended in 45 µl of Laemmli buffer with 0.2 M dithiothreitol, and the proteins were immunoblotted (14). Cell proliferation assays were performed as described (49). The C-loop β_3 F(ab)$_2$ antibody was added (10^{-9} M) immediately before the addition of IGF-1. Cell number was determined after 48 hours.

Induction of diabetes and antibody administration

Male Yorkshire pigs (12 months old; $n = 8$) were purchased from the Clemson University. They were maintained according to the *Guide for Care of Laboratory Animals* [National Institutes of Health (NIH) publication #85-23]. Eight pigs were placed on a high-fat diet containing 1% cholesterol, 20% beef tallow, and 0.75% cholic acid for 4 weeks. This diet induces increases in cholesterol and oxidized low-density lipoprotein (50). Vascular cholesterol deposits and foam cell deposition are detected after 8 weeks (50).

The animals received streptozotocin (50 mg/kg per day) intravenously for 3 days. Fasting glucose rose from 81 ± 11 mg/dl to 360 ± 123 mg/dl after 7 days. Two weeks later, all animals had catheters placed within the walls of both femoral arteries, with luminal opening placed into the arterial medial layer. The catheter was sutured into the adventitia, and a 2-ml Alzet minipump was placed in the subcutaneous space. The pump reservoir in one artery was filled with 2.0 ml of phosphate-buffered saline containing 0.7 mg of the C-loop β_3 F(ab)$_2$ antibody. The contralateral artery received 0.7 mg of control F(ab)$_2$. The locations of the treatments were randomized. Each artery received 23 µg per day for 30 days. A total of eight vessels received this dose of β_3 F(ab)$_2$ antibody and eight received the control. After 30 days, the pump reservoirs were exchanged and replacement solution of antibody was infused for an additional 30 days. This was continued for 3.5 months. This time interval was chosen because the investigators who developed this model showed that proliferative lesions developed over this interval and that a clear difference could be detected when diabetic and nondiabetic animals were compared (51).

Preparation of arteries for analysis

After euthanasia, femoral arteries were collected and processed as follows: (i) An open femoral artery was prepared for photography of raised atherosclerotic plaques; (ii) the section at the site of needle insertion was embedded in optimal cutting temperature (compound); (iii) the section distal to the needle insertion site was divided into 0.5-cm segments, frozen in liquid nitrogen, and stored at −80°C before biochemical analysis; and (iv) the segments proximal to the needle insertion site were placed in 10% buffered formalin and then 20 sections were taken at 50-µm intervals.

Morphometric analysis

Arterial sections were stained with Verhoeff–van Gieson to highlight the internal elastic lamina (IEL) and external elastic lamina (EEL). The image of each cross section was digitized and analyzed with an image analyzer (Nikon Microphot FXA microscope) with Optronics TEC 470CCD video camera system. Images of EEL, IEL, and lumen were captured and analyzed with NIH Image software (4, 17). The neointimal, luminal, and total cross-sectional areas were calculated. The neointimal area is the area inside the IEL minus the luminal area. The medial area is the total cross-sectional area minus the area inside the IEL. The observers were blinded as to treatment group. An average of 12 sections was analyzed per vessel. For statistical comparison of lesion area, the data were analyzed with two-way analysis of variance. Step-down tests, including *t* tests, were used for individual comparisons. To detect macrophages, we incubated the tissue sections with a 1:100 dilution of SRA-E5 (Cosmo Bio), a monoclonal antibody that detects the porcine macrophage scavenger receptor, for 1 hour at 22°C (4). This was followed by incubation with horse antibody to mouse IgG and Vectastain Elite avidin-biotin complex (ABC) reagents supplied in the Vectastain Universal Elite ABC kit (Vector Laboratories). The stain was visualized with NovaRED (Vector Laboratories) and counterstained with hematoxylin.

PCNA staining

Serial sections (5 μm thick) were obtained from paraffin-embedded vessels. Five sections per animal (every 10th section) was incubated with a 1:100 dilution of PCNA antibody (Dako) for 1 hour at 22°C followed by ABC Vectastain horse antibody to rabbit IgG secondary antibody. Staining was visualized with the chromogen diaminobenzidine (Vector Laboratories). The number of cells staining positive in the neointima was determined and expressed as a percentage of the total number of SMCs that were counted per section.

Biochemical analysis of arteries

Arterial samples were homogenized in modified RIPA buffer containing phosphatase and protease inhibitors (21). Protein abundances were determined with a bicinchoninic acid assay (Pierce). The procedures used for immunoprecipitation or immunoblotting of the tissue lysates were as described (21, 23).

Chemiluminescent images were scanned with a DuoScan T1200 (AGFA), and band intensities of the scanned images were analyzed with NIH Image version 1.61. The Student's *t* test was used to compare differences between treatments. The results that are shown are representative of at least three separate analyses.

Supplementary Material

Refer to Web version on PubMed Central for supplementary material.

Acknowledgments

REFERENCES AND NOTES

1. Bax JJ, Young LH, Frye RL, Bonow RO, Steinberg EJ. ADA, Screening for coronary artery disease in patients with diabetes. Diabetes Care. 2007; 30:2729–2736. [PubMed: 17901530]
2. Mikhailidis DP, Press M. The importance of treating multiple cardiometabolic risk factors in patients with type 2 diabetes. Expert Opin Pharmacother. 2007; 8:3009–3020. [PubMed: 18001259]

3. Zhu B, Zhao G, Witte DP, Hui DY, Fagin JA. Targeted overexpression of IGF-I in smooth muscle cells of transgenic mice enhances neointimal formation through increased proliferation and cell migration after intraarterial injury. Endocrinology. 2001; 142:3598–3606. [PubMed: 11459808]

4. Nichols TC, Busby WH Jr, Merricks E, Sipos J, Rowland M, Sitko K, Clemmons DR. Protease-resistant insulin-like growth factor (IGF)-binding protein-4 inhibits IGF-I actions and neointimal expansion in a porcine model of neointimal hyperplasia. Endocrinology. 2007; 148:5002–5010. [PubMed: 17640990]

5. Delafontaine P, Song YH, Li Y. Expression, regulation, and function of IGF-1, IGF-1R, and IGF-1 binding proteins in blood vessels. Arterioscler Thromb Vasc Biol. 2004; 24:435–444. [PubMed: 14604834]

6. Harrington SC, Simari RD, Conover CA. Genetic deletion of pregnancy-associated plasma protein-A is associated with resistance to atherosclerotic lesion development in apolipoprotein E–deficient mice challenged with a high-fat diet. Circ Res. 2007; 100:1696–1702. [PubMed: 17510462]

7. Pulai JI, Del Carlo M Jr, Loeser RF. The $\alpha 5\beta 1$ integrin provides matrix survival signals for normal and osteoarthritic human articular chondrocytes in vitro. Arthritis Rheum. 2002; 46:1528–1535. [PubMed: 12115183]

8. Zhong J, Deng J, Phan J, Dlouhy W, Wu H, Yao W, Ye P, D'Ercole AJ, Lee WH. Insulin-like growth factor-I protects granule neurons from apoptosis and improves ataxia in weaver mice. J Neurosci Res. 2005; 80:481–490. [PubMed: 15846777]

9. Hoshiga M, Alpers CE, Smith LL, Giachelli CM, Schwartz SM. $\alpha_v\beta_3$ integrin expression in normal and atherosclerotic artery. Circ Res. 1995; 77:1129–1135. [PubMed: 7586225]

10. Giachelli CM, Bae N, Almeida M, Denhardt DT, Alpers CE, Schwartz SM. Osteopontin is elevated during neointima formation in rat arteries and is a novel component of human atherosclerotic plaques. J Clin Invest. 1993; 92:1686–1696. [PubMed: 8408622]

11. Bhattacharyya S, Marinic TE, Krukovets I, Hoppe G, Stenina OI. Cell type-specific post-transcriptional regulation of production of the potent antiangiogenic and proatherogenic protein thrombospondin-1 by high glucose. J Biol Chem. 2008; 283:5699–5707. [PubMed: 18096704]

12. Mori S, Takamoto M, Yokote K, Asaumi S, Saito Y. Hyperglycemia-induced alteration of vascular smooth muscle phenotype. J Diabetes Complications. 2002; 16:65–68. [PubMed: 11872370]

13. Jones JI, Prevette T, Gockerman A, Clemmons DR. Ligand occupancy of the α-V-β3 integrin is necessary for smooth muscle cells to migrate in response to insulin-like growth factor. Proc Natl Acad Sci USA. 1996; 93:2482–2487. [PubMed: 8637900]

14. Maile LA, Capps BE, Ling Y, Xi G, Clemmons DR. Hyperglycemia alters the responsiveness of smooth muscle cells to insulin-like growth factor-I. Endocrinology. 2007; 148:2435–2443. [PubMed: 17255202]

15. Zheng B, Clemmons DR. Blocking ligand occupancy of the $\alpha V\beta 3$ integrin inhibits insulin-like growth factor I signaling in vascular smooth muscle cells. Proc Natl Acad Sci USA. 1998; 95:11217–11222. [PubMed: 9736716]

16. Srivatsa SS, Fitzpatrick LA, Tsao PW, Reilly TM, Holmes DR Jr, Schwartz RS, Mousa SA. Selective $\alpha v\beta 3$ integrin blockade potently limits neointimal hyperplasia and lumen stenosis following deep coronary arterial stent injury: Evidence for the functional importance of integrin $\alpha v\beta 3$ and osteopontin expression during neointima formation. Cardiovasc Res. 1997; 36:408–428. [PubMed: 9534862]

17. Nichols TC, du Laney T, Zheng B, Bellinger DA, Nickols GA, Engleman W, Clemmons DR. Reduction in atherosclerotic lesion size in pigs by $\alpha V\beta 3$ inhibitors is associated with inhibition of insulin-like growth factor-I–mediated signaling. Circ Res. 1999; 85:1040–1045. [PubMed: 10571535]

18. Maubant S, Saint-Dizier D, Boutillon M, Perron-Sierra F, Casara PJ, Hickman JA, Tucker GC, Van Obberghen-Schilling E. Blockade of $\alpha V\beta 3$ and $\alpha V\beta 5$ integrins by RGD mimetics induces anoikis and not integrin-mediated death in human endothelial cells. Blood. 2006; 108:3035–3044. [PubMed: 16835373]

19. Monleón D, Esteve V, Kovacs H, Calvete JJ, Celda B. Conformation and concerted dynamics of the integrin-binding site and the C-terminal region of echistatin revealed by homonuclear NMR. Biochem J. 2005; 38:57–66. [PubMed: 15535803]

20. Hu DD, Barbas CF, Smith JW. An allosteric CA^{2+} binding site on the β3-integrins that regulates the dissociation rate for RGD ligands. J Biol Chem. 1996; 271:21745–21751. [PubMed: 8702970]

21. Maile LA, Busby WH, Sitko K, Capps BE, Sergent T, Badley-Clarke J, Ling Y, Clemmons DR. Insulin-like growth factor-I signaling in smooth muscle cells is regulated by ligand binding to the ^{177}CYDMKTTC^{184} sequence of the β3-subunit of αVβ3. Mol Endocrinol. 2006; 20:405–413. [PubMed: 16195248]

22. Xiong JP, Stehle T, Zhang R, Joachimiak A, Frech M, Goodman SL, Arnaout MA. Crystal structure of the extracellular segment of integrin αVβ3 in complex with an Arg-Gly-Asp ligand. Science. 2002; 296:151–155. [PubMed: 11884718]

23. Maile LA, Busby WH, Sitko K, Capps BE, Sergent T, Badley-Clarke J, Ling Y, Clemmons DR. The heparin binding domain of vitronectin is the region that is required to enhance insulin-like growth factor-I signaling. Mol Endocrinol. 2006; 20:881–892. [PubMed: 16322097]

24. Choi ET, Khan MF, Leidenfrost JE, Collins ET, Boc KP, Villa BR, Novack DV, Parks WC, Abendschein DR. β$_3$-Integrin mediates smooth muscle cell accumulation in neointima after carotid ligation in mice. Circulation. 2004; 109:1564–1569. [PubMed: 15007005]

25. Stouffer GA, Hu Z, Sajid M, Li H, Jin G, Nakada MT, Hanson SR, Runge MS. β$_3$ Integrins are upregulated after vascular injury and modulate thrombospondin- and thrombin-induced proliferation of cultured smooth muscle cells. Circulation. 1998; 97:907–915. [PubMed: 9521340]

26. Janat MF, Argraves WS, Liau G. Regulation of vascular smooth muscle cell integrin expression by transforming growth factor β1 and by platelet-derived growth factor-BB. J Cell Physiol. 1992; 151:588–595. [PubMed: 1295906]

27. Blindt R, Bosserhoff AK, Zeiffer U, Krott N, Hanrath P, vom Dahl J. Abciximab inhibits the migration and invasion potential of human coronary artery smooth muscle cells. J Mol Cell Cardiol. 2000; 32:2195–2206. [PubMed: 11112995]

28. Topol EJ, Lincoff AM, Kereiakes DJ, Kleiman NS, Cohen EA, Ferguson J, Tcheng JE, Sapp S, Califf RM. Multi-year follow-up of abciximab therapy in three randomized, placebo-controlled trials of percutaneous coronary revascularization. Am J Med. 2002; 113:1–6. [PubMed: 12106616]

29. Huang Q, Sheibani N. High glucose promotes retinal endothelial cell migration through activation of Src, PI3K/Akt1/eNOS, and ERKs. Am J Physiol Cell Physiol. 2008; 295:C1647–C1657. [PubMed: 18945941]

30. Ning A, Cui J, Maberley D, Ma P, Matsubara J. Expression of integrins in human proliferative diabetic retinopathy membranes. Can J Ophthalmol. 2008; 43:683–688. [PubMed: 19020635]

31. Belmadani S, Zerfaoui M, Boulares HA, Palen DI, Matrougui K. Microvessel vascular smooth muscle cells contribute to collagen type I deposition through ERK1/2 MAP kinase, αvβ$_3$-integrin, and TGF-β1 in response to ANG II and high glucose. Am J Physiol Heart Circ Physiol. 2008; 295:H69–H76. [PubMed: 18456735]

32. Sodhi CP, Phadke SA, Batlle D, Sahai A. Hypoxia and high glucose cause exaggerated mesangial cell growth and collagen synthesis: Role of osteopontin. Am J Physiol Renal Physiol. 2001; 280:F667–F674. [PubMed: 11249858]

33. Wahab NA, Schaefer L, Weston BS, Yiannikouris O, Wright A, Babelova A, Schaefer R, Mason RM. Glomerular expression of thrombospondin-1, transforming growth factor β and connective tissue growth factor at different stages of diabetic nephropathy and their interdependent roles in mesangial response to diabetic stimuli. Diabetologia. 2005; 48:2650–2660. [PubMed: 16270194]

34. Danda RS, Habiba NM, Rincon-Choles H, Bhandari BK, Barnes JL, Abboud HE, Pergola PE. Kidney involvement in a nongenetic rat model of type 2 diabetes. Kidney Int. 2005; 68:2562–2571. [PubMed: 16316331]

35. Bhattacharyya S, Marinic TE, Krukovets I, Hoppe G, Stenina OI. Cell type-specific post-transcriptional regulation of production of the potent antiangiogenic and proatherogenic protein thrombospondin-1 by high glucose. J Biol Chem. 2008; 283:5699–5707. [PubMed: 18096704]

36. Ling Y, Maile LA, Clemmons DR. Tyrosine phosphorylation of the β3-subunit of the αVβ3 integrin is required for membrane association of the tyrosine phosphatase SHP-2 and its further recruitment to the insulin-like growth factor I receptor. Mol Endocrinol. 2003; 17:1824–1833. [PubMed: 12791772]

37. Sodhi CP, Phadke SA, Batlle D, Sahai A. Hypoxia stimulates osteopontin expression and proliferation of cultured vascular smooth muscle cells: Potentiation by high glucose. Diabetes. 2001; 50:1482–1490. [PubMed: 11375351]

38. Campbell M, Allen WE, Silversides JA, Trimble ER. Glucose-induced phosphatidylinositol 3-kinase and mitogen-activated protein kinase-dependent upregulation of the platelet-derived growth factor-β receptor potentiates vascular smooth muscle cell chemotaxis. Diabetes. 2003; 52:519–526. [PubMed: 12540630]

39. Cercek B, Fishbein MC, Forrester JS, Helfant RH, Fagin JA. Induction of insulin-like growth factor I messenger RNA in rat aorta after balloon denudation. Circ Res. 1990; 66:1755–1760. [PubMed: 2188750]

40. Khorsandi M, Fagin JA, Fishbein MC, Forrester JS, Cercek B. Effects of hypophysectomy on vascular insulin-like growth factor-I gene expression after balloon denudation in rats. Atherosclerosis. 1992; 93:115–122. [PubMed: 1596294]

41. Grant MB, Wargovich TJ, Ellis EA, Caballero S, Mansour M, Pepine CJ. Localization of insulin-like growth factor I and inhibition of coronary smooth muscle cell growth by somatostatin analogues in human coronary smooth muscle cells. A potential treatment for restenosis? Circulation. 1994; 89:1511–1517. [PubMed: 7908609]

42. Du J, Peng T, Scheidegger KJ, Delafontaine P. Angiotensin II activation of insulin-like growth factor 1 receptor transcription is mediated by a tyrosine kinase-dependent redox-sensitive mechanism. Arterioscler Thromb Vasc Biol. 1999; 19:2119–2126. [PubMed: 10479653]

43. Häyry P, Myllärniemi M, Aavik E, Alatalo S, Aho P, Yilmaz S, Räisänen-Sokolowski A, Cozzone G, Jameson BA, Baserga R. Stabile D-peptide analog of insulin-like growth factor-1 inhibits smooth muscle cell proliferation after carotid ballooning injury in the rat. FASEB J. 1995; 9:1336–1344. [PubMed: 7557024]

44. Garcia-Segura LM, Sanz A, Mendez P. Cross-talk between IGF-I and estradiol in the brain: Focus on neuroprotection. Neuroendocrinology. 2006; 84:275–279. [PubMed: 17124377]

45. Wittman M, Carboni J, Attar R, Balasubramanian B, Balimane P, Brassil P, Beaulieu F, Chang C, Clarke W, Dell J, Eummer J, Frennesson D, Gottardis M, Greer A, Hansel S, Hurlburt W, Jacobson B, Krishnananthan S, Lee FY, Li A, Lin TA, Liu P, Ouellet C, Sang X, Saulnier MG, Stoffan K, Sun Y, Velaparthi U, Wong H, Yang Z, Zimmermann K, Zoeckler M, Vyas D. Discovery of a (1*H*-benzoimidazol-2-yl)-1*H*-pyridin-2-one (BMS-536924) inhibitor of insulin-like growth factor I receptor kinase with in vivo antitumor activity. J Med Chem. 2005; 48:5639–5643. [PubMed: 16134929]

46. Li Y, Higashi Y, Itabe H, Song YH, Du J, Delafontaine P. Insulin-like growth factor-1 receptor activation inhibits oxidized LDL-induced cytochrome C release and apoptosis via the phosphatidylinositol 3 kinase/Akt signaling pathway. Arterioscler Thromb Vasc Biol. 2003; 23:2178–2184. [PubMed: 14551153]

47. Gockerman A, Prevette T, Jones JI, Clemmons DR. Insulin-like growth factor (IGF)-binding proteins inhibit the smooth muscle cell migration responses to IGF-I and IGF-II. Endocrinology. 1995; 136:4168–4173. [PubMed: 7545099]

48. Bonroy K, Frederix F, Reekmans G, Dewolf E, De Palma R, Borghs G, Declerk P, Goddeeris B. Comparison of random and oriented immobilisation of antibody fragments on mixed self-assembled monolayers. J Immunol Methods. 2006; 312:167–181. [PubMed: 16674973]

49. Nam TJ, Busby WH Jr, Rees C, Clemmons DR. Thrombospondin and osteopontin bind to insulin-like growth factor (IGF)-binding protein-5 leading to an alteration in IGF-I-stimulated cell growth. Endocrinology. 2000; 141:1100–1106. [PubMed: 10698186]

50. Griggs TR, Bauman RW, Reddick RL, Read MS, Koch GG, Lamb MA. Development of coronary atherosclerosis in swine with severe hypercholesterolemia. Lack of influence of von Willebrand factor or acute intimal injury. Arteriosclerosis. 1986; 6:155–165. [PubMed: 3485423]

51. Gerrity RG, Natarajan R, Nadler JL, Kimsey T. Diabetes-induced accelerated atherosclerosis in swine. Diabetes. 2001; 50:1654–1665. [PubMed: 11423488]
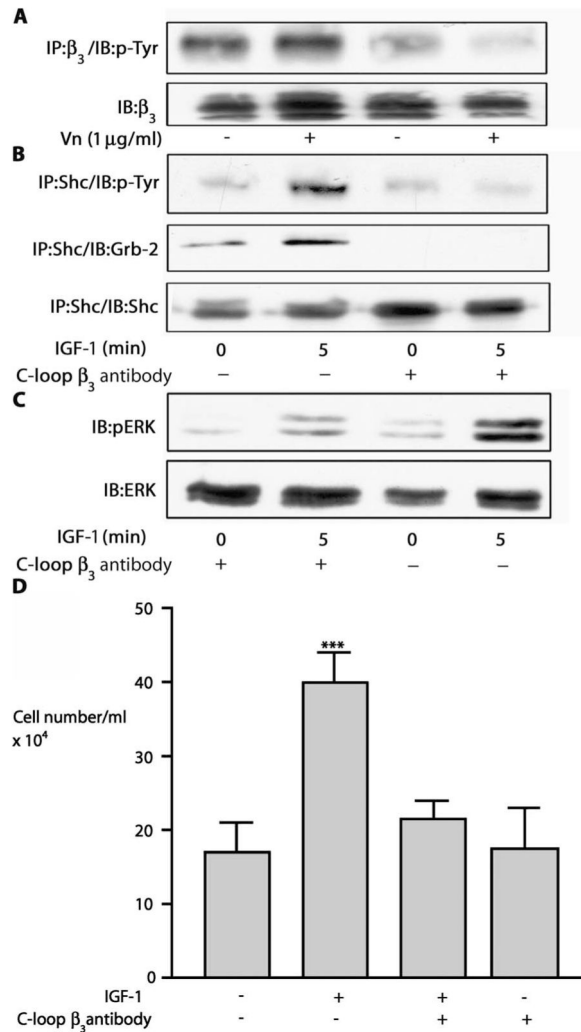
Fig. 1.
Effect of F(ab)$_2$ against C-loop of β_3 on IGF-1 signaling events. (**A**) SMCs were exposed to the C-loop β_3 F(ab)$_2$ (10^{-9} M) for 2 hours before a further 2-hour incubation with vitronectin (Vn) (1 µg/ml). After immunoprecipitation (IP) with antibody to β_3, β_3 phosphorylation was visualized by immunoblotting (IB) with an antibody to phosphotyrosine (p-Tyr). Lysates were also immunoblotted directly with an antibody to β_3 to control for differences in protein loading. (**B**) Cells were treated with or with-out the C-loop β_3 F(ab)$_2$ (10^{-9} M) for 4 hours followed by IGF-1 (50 ng/ml). Shc phosphorylation was determined by immunoprecipitation with an antibody to Shc and immunoblotting with an antibody to phosphotyrosine (top). Shc association with Grb-2 was determined by immunoprecipitation with an antibody to Shc and immunoblotting with an antibody to Grb-2 (middle). To control for loading, we reprobed blots with an antibody to Shc (bottom). (**C**) SMCs were treated with or without C-loop β_3 F(ab)$_2$ (10^{-9} M) for 4 hours followed by the addition of IGF-1 (50 ng/ml). After lysis, proteins were separated by SDS-PAGE before immunoblotting with an antibody to phospho-ERK1/2 (pERK) or total ERK. (**D**) SMCs (2×10^4) were plated in each well of a 24-well plate before exposure to IGF-1 (50 ng/ml) in the presence or absence of the C-loop β_3 F(ab)$_2$ (10^{-9} M). After 48 hours, cell number was determined. ***$P < 0.001$ when proliferation in the presence of IGF-1 is compared with control.
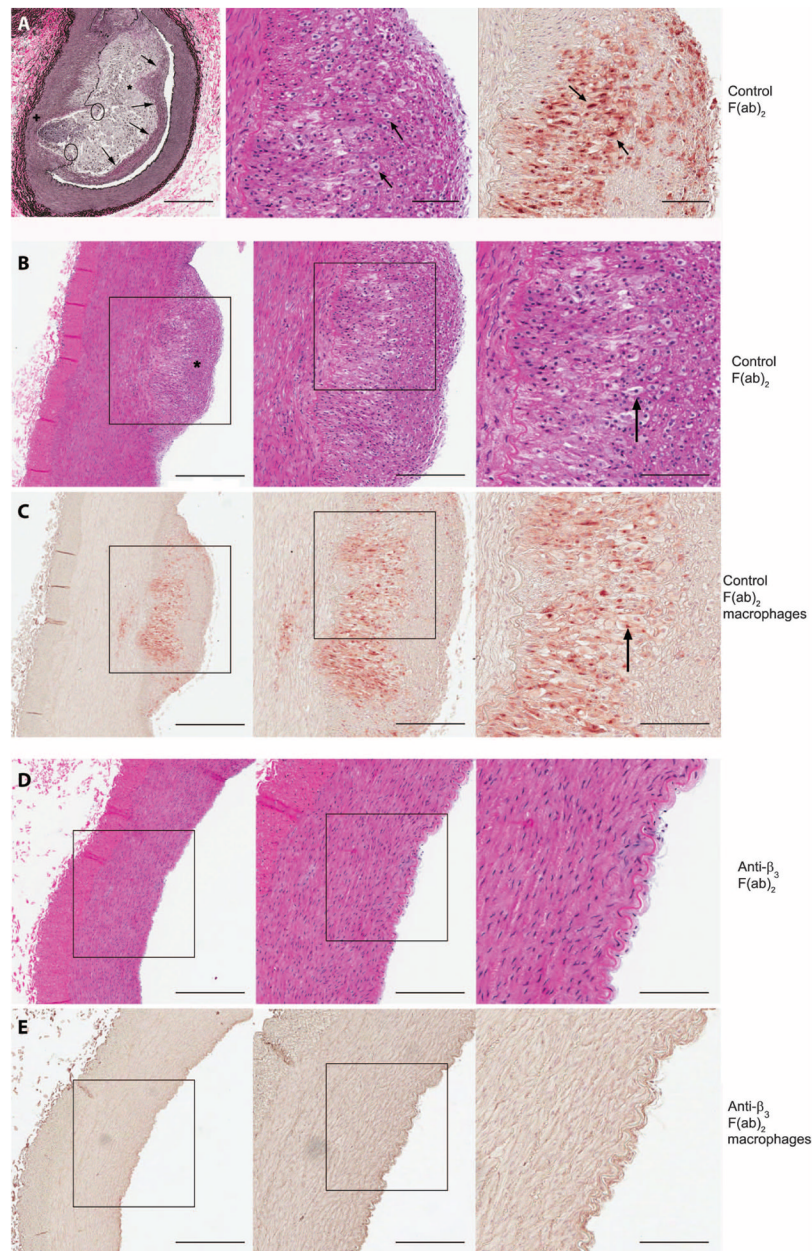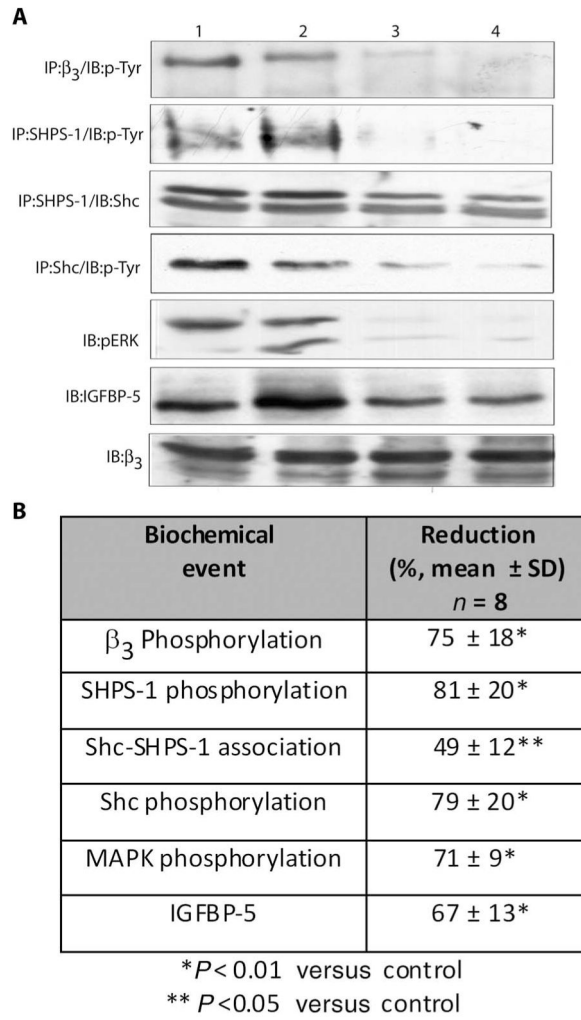
Fig. 2.

Photomicrographs of the atherosclerotic lesions. (**A**) Features of atherosclerotic plaques in femoral arteries treated with control F(ab)$_2$. Left, Verhoeff–van Gieson stain. Arrows, fibrous cap; asterisk, necrotic cells; circles, disrupted IEL + medial thinning. Scale bars, 400 μm (left) and 100 μm (middle and right). Middle, hematoxylin and eosin (H&E) stain. Arrows, foam cells. Right, stained with antibody to macrophage scavenger receptor (SRA-35). Arrows, positively stained cells. (**B**) A control artery from a different animal. Left, stained with H&E. Asterisk, well-developed fibrous cap. Middle, enlargement of same areas as in the left panel. Right, enlargement of boxed area in middle panel. Arrow, foam cell. (**C**) Sections adjacent to these shown in (B) stained with antibody to macrophage scavenger. Middle, enlargement of left panel. Right, boxed area from middle panel. Arrows, positively stained cells. (**D**) A F(ab)$_2$ anti-β$_3$–treated artery from the same animal as shown

in (A) stained with H&E. (**E**) Sections from the same artery stained with the antibody to macrophage scavenger receptor. No macrophages were detected in the artery treated with F(ab)$_2$ antibody to β_3. (B to E) Scale bars, 500 μm (left), 250 μm (middle), and 125 μm (right).

A

B

Biochemical event	Reduction (%, mean ± SD) $n = 8$
β_3 Phosphorylation	75 ± 18*
SHPS-1 phosphorylation	81 ± 20*
Shc-SHPS-1 association	49 ± 12**
Shc phosphorylation	79 ± 20*
MAPK phosphorylation	71 ± 9*
IGFBP-5	67 ± 13*

*$P < 0.01$ versus control
** $P < 0.05$ versus control

Fig. 3.
Effect of infusion of F(ab)$_2$ against the C-loop of β_3 on IGF signaling events in porcine arteries. (**A**) Tissue homogenates from the femoral arteries were either directly immunoblotted with the appropriate antibody or used for immunoprecipitation before SDS-PAGE and immunoblotting. The proteins that were detected are listed in the left panel. Lanes 1 and 2, lesion homogenates from arteries that received control F(ab)$_2$; lanes 3 and 4, lesion homogenates from arteries that received the C-loop F(ab)$_2$ antibody to β_3. (**B**) The table shows the mean ± SD results from all eight animals.

Table 1

Changes in metabolic parameters.

	Induction of diabetes	Start of treatment	1 Month	2 Months	3 Months
Weight (lbs)	$180 \pm 11^*$	220 ± 15	231 ± 21	$256 \pm 23^\dagger$	$266 \pm 29^\dagger$
Cholesterol (mg/dl)	87 ± 7	731 ± 154	800 ± 170	674 ± 102	598 ± 96
Triglycerides (mg/dl)	31 ± 3	67 ± 10	$175 \pm 43^\dagger$	$169 \pm 69^\dagger$	$132 \pm 50^\dagger$
Glucose (mg/dl)‡	62 ± 6	340 ± 94	368 ± 71	360 ± 88	348 ± 85
Insulin dose (U/day)	ND	27 ± 12	24 ± 8	23 ± 10	28 ± 12

*
Each value represents the mean ($n = 8$) ± SD.

† $P < 0.05$ relative to the values at the start of antibody treatment.

‡ Each glucose value represents the mean of four measurements per animal per 24-hour interval.

Table 2

Morphometric analysis of femoral arteries.

Treatment	Vessels (n)	Intimal area, μm^2 (mean $\pm$ SD)	Intimal area, % of medial area (mean $\pm$ SD)	% PCNA
F(ab)$_2$ antibody to β_3	8	59,438 $\pm$ 7,132[*]	9.3 $\pm$ 2.8[†]	3.1 $\pm$ 4.2%[*]
Control	8	132,086 $\pm$ 19,041	21.1 $\pm$ 3.2	19.3 $\pm$ 3.7%

[*]$P < 0.01$ versus control.

[†]$P < 0.05$ versus control.